Dynamics of Atmospheres and Oceans 80 (2017) 124–138

Contents lists available at ScienceDirect

Dynamics of Atmospheres and Oceans

journal homepage: www.elsevier.com/locate/dynatmoce

Observations and operational model simulations reveal the impact of Hurricane Matthew (2016) on the Gulf Stream and coastal sea level

Tal Ezer*, Larry P. Atkinson, Robert Tuleya

Center for Coastal Physical Oceanography, Old Dominion University, 4111 Monarch Way, Norfolk, VA, 23508, USA

ARTICLE INFO

Article history:
Received 2 March 2017
Received in revised form 18 July 2017
Accepted 25 October 2017

Keywords:
Coastal currents
Sea level
Hurricanes
Flooding
Gulf stream
Florida current

ABSTRACT

In October 7–9, 2016, Hurricane Matthew moved along the southeastern coast of the U.S., causing major flooding and significant damage, even to locations farther north well away from the storm's winds. Various observations, such as tide gauge data, cable measurements of the Florida Current (FC) transport, satellite altimeter data and high-frequency radar data, were analyzed to evaluate the impact of the storm. The data show a dramatic decline in the FC flow and increased coastal sea level along the U.S. coast. Weakening of the Gulf Stream (GS) downstream from the storm's area contributed to high coastal sea levels farther north. Analyses of simulations of an operational hurricane-ocean coupled model reveal the disruption that the hurricane caused to the GS flow, including a decline in transport of ~20 Sv (1 Sv = 10^6 m^3 s^{-1}). In comparison, the observed FC reached a maximum transport of ~40 Sv before the storm on September 10 and a minimum of ~20 Sv after the storm on October 12. The hurricane impacts both the geostrophic part of the GS and the wind-driven currents, generating inertial oscillations with velocities of up to ±1 m s^{-1}. Analysis of the observed FC transport since 1982 indicated that the magnitude of the current weakening in October 2016 was quite rare (outside 3 standard deviations from the mean). Such a large FC weakening in the past occurred more often in October and November, but is extremely rare in June-August. Similar impacts on the FC from past tropical storms and hurricanes suggest that storms may contribute to seasonal and interannual variations in the FC. The results also demonstrated the extended range of coastal impacts that remote storms can cause through their influence on ocean currents.

1. Introduction

Hurricane Matthew developed in the Caribbean in late September 2016, and quickly intensified from category 1–5 (maximum wind of 260 km h^{-1}), before weakening to category 3–4 when moving northward across Cuba and Haiti and causing significant damage and loss of life. During October 7–9 the hurricane moved along the coasts of Florida, Georgia, South Carolina and North Carolina, before looping east and dissipating. The southeastern States suffered several billions of dollars of damages, mostly due to large amount of rain and storm surge flooding (see the National Hurricane Center, http://www.nhc.noaa.gov/, and various weather news reports such as

* Corresponding author.
E-mail address: tezer@odu.edu (T. Ezer).

https://doi.org/10.1016/j.dynatmoce.2017.10.006
0377-0265/

https://weather.com/storms/hurricane/news/hurricane-matthew-bahamas-florida-georgia-carolinas-forecast). Tide gauge data along the storm passage show that storm surges reached water levels of ~1–1.5 m in Fernandina, FL, Pulasky, GA, Charleston, SC, and Wilmington, NC (all levels are relative to Mean Higher High Water, MHHW). However, somewhat surprising was that water levels farther away from the storm were also raised significantly, for example to ~1 m (MHHW) in Norfolk, VA, and 0.3–0.5 m in other locations in the Chesapeake Bay and the Atlantic coast (as far as the New Jersey coast, as shown later). Significant flood damage to houses in Virginia Beach may be attributed to street flooding due to extreme rainfall that could not drain because sea levels were high at the same time. Interestingly enough, a similar phenomenon of high water levels in Norfolk happened a year earlier (September–October 2015) when hurricane Joaquin was located well offshore- details of the sea level during this storm was reported in a recent study (Ezer and Atkinson, 2017). This latter study also demonstrated some predictability skill in using the Florida Current measurements to infer high water levels in Norfolk.

One possible hypothesis for how a remote storm can influence coastal sea level along the U.S. East Coast is through the impact of the storm on the Gulf Stream (GS). Weakening in a western boundary current transport will decrease the seaward sea level slope across the current (i.e., the GS) and increase coastal sea level on the onshore side of the current; this idea was suggested decades ago (Blaha, 1984) and confirmed by recent observations (Ezer et al., 2013, Ezer and Atkinson, 2014, 2017; Ezer, 2015, 2016) and numerical models (Ezer, 2001, 2016; Goddard et al., 2015). On long time-scales, studies suggest that recent sea level acceleration on the U.S. East Coast may be partly driven by climate-related slowdown of the Atlantic Meridional Overturning Circulation (AMOC) (McCarthy et al., 2012; Smeed et al., 2013) and a weakening Gulf Stream (Boon, 2012; Ezer and Corlett, 2012; Sallenger et al., 2012; Ezer et al., 2013). However, these long-term variations in the GS are relatively small and involve also basin-scale decadal and longer variations that are not directly related to coastal sea level. On the other hand, large short-term fluctuations in the GS transport (order of ~5–10 SV within few days) are quite common, and there is growing evidence that these variations can be detected within days in coastal sea level records. The short-term variations can cause unexpected tidal flooding even when there is no storm nearby (Ezer and Atkinson, 2014; Park and Sweet, 2015; Wdowinski et al., 2016). The mechanism of this observed short-term sea level-GS correlation (with very short lag of hours to few days) was recently explored by numerical simulations (Ezer, 2016). The simulations demonstrated how variations in the FC transport with periods of 2–10 days can create a fast moving barotropic signal downstream along the GS path that then ignites coastal trapped waves that result in coherent sea level variations along long stretches of the U.S. East coast. It should be noted that while the focus of our study is on the portion of coastal sea level variability that is contributed by ocean dynamics, impact from variations in wind and atmospheric pressure (through the inverted barometer effect, IB) are of course, very significant. IB variability on interannual and multidecadal time scales may contribute as much as 10–30% of the sea level signal (Piecuch and Ponte, 2015) and wind plays a major role on these scales as well (Piecuch et al., 2016; Woodworth et al., 2016). IB and wind could play even larger roles in short time scales associated with tropical storms and hurricanes.

The impact of storms and hurricanes on the ocean is often focused on the heat loss and the cooling effect of surface temperatures (Bender and Ginis, 2000; Shay et al., 2000; Li et al., 2002; Oey et al., 2006, 2007; Yablonsky et al., 2015), while less attention is given to the impact on ocean currents. Some modeling studies demonstrate that hurricanes can significantly alter even strong ocean currents: for example, Hurricane Wilma (2005) caused intensification of the Loop Current (Oey et al., 2006), while Hurricane Bill (2009) created a large temporary reduction of the GS transport north of Cape Hatteras associated with deepening of the mixed layer and reduction of stratification (Kourafalou et al., 2016); the latter study found similar impacts from several other hurricanes. Winter storms moving over the warm GS can also have significant impact on both air-sea heat fluxes and GS currents (Li et al., 2002). Note that while the focus here is on the interaction of Atlantic Ocean hurricanes with the Gulf Stream, similar interactions between Pacific Ocean Typhoons and the Kuroshio have also been studied (Wu et al., 2008; Liu and Wei, 2015), so influence from storms on western boundary currents and ocean circulation may be an important issue for further research.

In this study, several direct and remote sensing data sources, as well as simulations from an operational hurricane-ocean coupled model, are analyzed to reveal the impact of Hurricane Matthew (2016) on ocean currents and coastal sea level. In particular, the goal is to focus not only on the direct impact of wind-driven storm surges which are quite well studied, but also study potential indirect mechanisms where strong ocean currents are altered by the storm and then can influence coastal sea level.

2. Data and models

Hourly water level records from tide gauge data along the U.S. coast were obtained from NOAA (http://opendap.co-ops.nos.noaa.gov/dods/). These records have been used for various studies of sea level rise (Boon, 2012; Ezer and Corlett, 2012; Ezer, 2013). When calculating non-tidal daily values of WL anomalies from the hourly data, errors are estimated to be around ±5–10 cm (i.e., values are expected to be within mean ± error 95% of the time), and the higher values were used during storms. The daily Florida Current (FC) transport has been available since March 1982 (with a major gap in data from October 1998 to June 2000) using the cable measurements across the Florida Strait at ~27°N (Baringer and Larsen 2001; Meinen et al., 2010). The FC cable data are available on the Atlantic Oceanographic and Meteorological Laboratory web page (www.aoml.noaa.gov/phod/floridacurrent/) and are funded by the DOC—NOAA Climate Program Office-Climate Observation Division. NOAA reports in this web site indicate quite unchanged error bars in the daily value, about ±1.6 Sv. The FC transport experienced seasonal and interannual variability, as well as modulations due

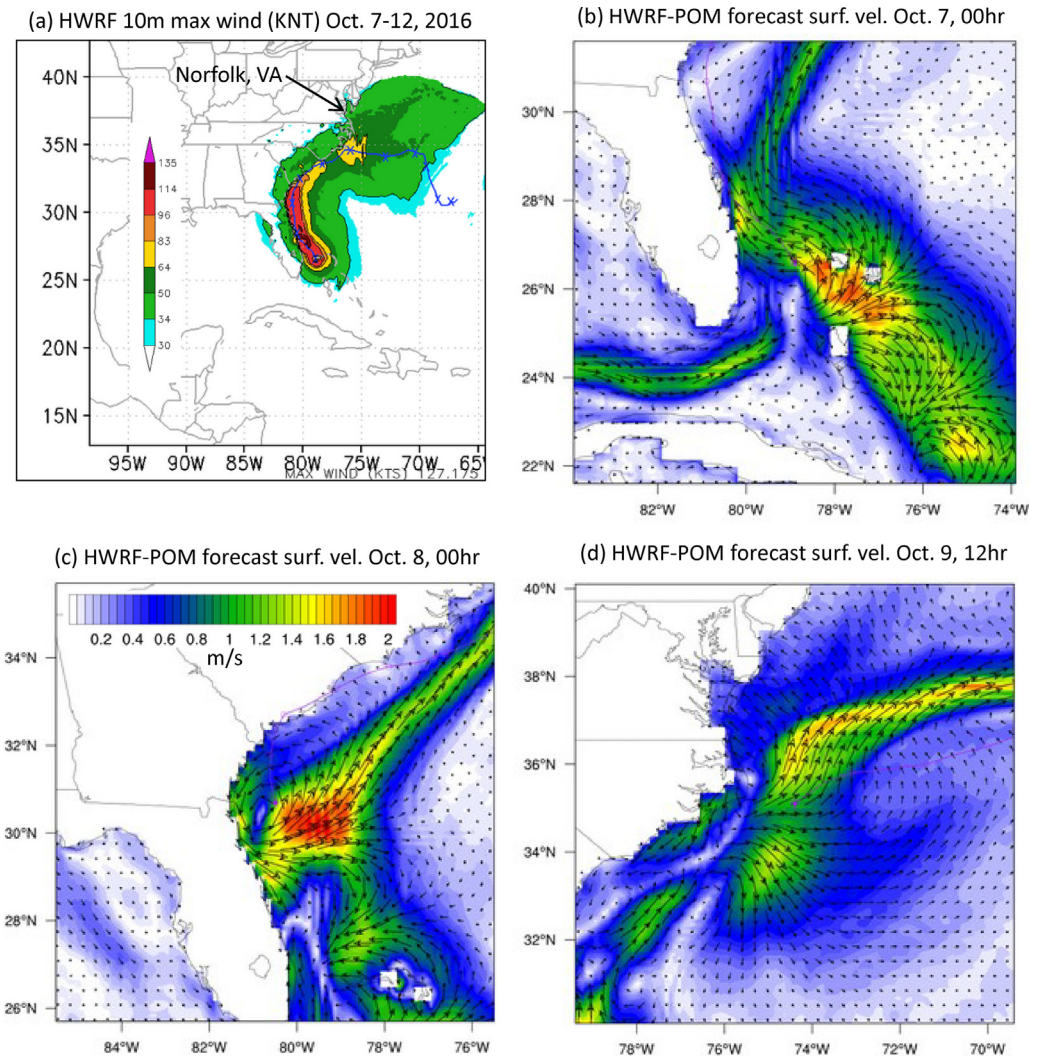

Fig. 1. The operational forecast of the HWRF-POM model for Hurricane Matthew: (a) storm predicted track ("x" and blue line) and maximum wind field (color in knots) for October 7–12, 2016; (b)–(d) are the surface ocean currents (vector for direction and color for speed) for October 7, 8 and 9, respectively (data from http://www.emc.ncep.noaa.gov/gc_wmb/vxt/HWRF/). (For interpretation of the references to colour in this figure legend, the reader is referred to the web version of this article.)

to remote Atlantic Ocean forcing (Domingues et al., 2016). However, short-term variability associated with tropical storms and hurricanes has not been given much attention so far. The composite gridded satellite altimeter data were obtained from AVISO (http://las.aviso.oceanobs.com/; AVISO, 2009). The Coastal Ocean Dynamics Applications Radar (CODAR) is a land-based high-frequency (HF) radar with several stations distributed along the U.S. East Coast. Description and evaluation of the radar data are found in Kohut et al. (2012), which found errors of surface velocities in these measurements to be around $\pm 8\,\mathrm{cm\,s^{-1}}$.

To study the ocean response to hurricanes from a model perspective, output from NOAA's coupled operational Hurricane Weather Research and Forecasting (HWRF) model (Yablonsky et al., 2015; Tallapragada et al., 2014) was utilized (using the version available at the time of the storm, version MPIPOM-TC:MATTHEW14L). The Princeton Ocean Model (POM) component of the coupled system has horizontal resolution of 7–9 km and 23 vertical terrain-following layers with higher resolution near the surface; the model domain covers the western North Atlantic Ocean (10°N–47.5°N, 30°W–100°W). Vertical mixing is provided by a Mellor-Yamada turbulence model. Observations are combined with feature-based models to provide initial conditions that represent the Loop Current, the Gulf Stream and some mesoscale eddies in a more realistic way than monthly climatology (see Yablonsky et al., 2015, for details). While the feature model initialization is quite idealized, it nevertheless provides subsurface information that was not available in past hurricane prediction models that used only sea surface temperature to represent the ocean. Assimilation of surface observed temperatures is done during a spin up period, before the operational forecast started. Six-hour operational forecast fields of hurricane Matthew from HWRF originating from October 7 and extending to October 12, 2016 were used. Fig. 1 shows the path of the hurricane and the HWRF-

POM forecasted winds and surface currents during this period. This hurricane had an unusual track (Fig. 1a), hugging the southeastern coast and then looping clockwise back offshore, in contrast with tracks of many other storms that often continue straight toward the coast; this track thus caused the hurricane to spend several days in the vicinity of the Gulf Stream, which may have resulted in a strong impact on the Gulf Stream current, as discussed later. Inaccuracies in the representation of eddies, errors in predicting the model track and hurricane intensity will add to discrepancies between observed and predicted sea level, as shown later. While evaluation of the hurricane model itself is beyond the scope of this study, the focus here is on the impact of the hurricane on the GS and on sea level. It is quite clear that the hurricane's winds affect surface currents near the GS (Fig. 1b–d), but does the hurricane have an impact on the subsurface fields and does this impact last beyond the few days (October 7–9) that the hurricane was close to shore? These questions will be explored using the various data described above.

3. Results

3.1. Impact of Hurricane Matthew on coastal sea level

The motivation for this study comes from the recent discovery that unusually high water levels in the Mid-Atlantic Bight, and in particular near Norfolk, VA, often occur on clear days without any nearby storm, but when the GS suddenly weakens (Ezer and Atkinson, 2014, 2017; Ezer, 2016). This phenomenon can cause minor tidal flooding or make storm surges more destructive. There are many different reasons for variations in the GS as measured by the FC cable (Baringer and Larsen, 2001; Meinen et al., 2010; Domingues et al., 2016). There are ~3–4 Sv annual cycles and 2–3 Sv interannual and decadal variations. However, these normal variations occur over long timescales and are an order of magnitude smaller than the ~10–20 Sv changes seen for example during a few days in October 2016. The impact of hurricanes on the GS is not widely discussed, though it has been recently suggested to be significant (Kourafalou et al., 2016). Water level (WL relative to MHHW) in Norfolk over a 3-months period (August to October 2016; Fig. 2a) was ~20–50 cm above the NOAA's predicted tide most of this time, with particularly high water during the time when two hurricanes and a tropical storm were offshore in the Atlantic. It is possible that several storms passing over the same region within a relatively short period of time would have an accumulating impact on ocean mixing. For example, even though the sea level response in Norfolk to weaker storms, such as Julia is quite small, it adds to the mixing caused by the stronger hurricanes, and may contribute to the FC decline seen over several weeks. Because the coastal sea level response to short-term variations in the GS is seen within short period of time (hours to few days) as reported before (Ezer and Atkinson, 2014, 2017; Ezer, 2016), it is difficult to separate between the direct storm surge impact and indirect GS-related variations. Analysis (shown later) of geostrophic versus wind-driven contributions to the GS flow may shed further light on the dynamics and the direct contribution of the wind. Note that due to sea level rise, today some streets in Norfolk start to be covered with water during high tides when WL is only ~30 cm over MHHW (Ezer and Atkinson, 2014). These three storms in Fig. 2a were hundreds of kilometers away from Norfolk, so the rise of water level was mainly attributed to the indirect effects of the storms and not from local wind-driven storm surges. The observed FC transport across the Florida Straits (blue line in Fig. 2b) shows a dramatic decrease from ~40 Sv in mid September to ~20 Sv in mid October, with the largest decline during a few days when hurricane Matthew was near the Florida coast. The large FC weakening over several weeks is probably the result of accumulating impacts from several storms in addition to possible natural variations. The WL anomaly is anti-correlated with the FC transport (Fig. 2b) and with the change in the FC transport (Fig. 2c). Note that although the FC-sea level correlation of −0.5 is statistically significant at 99% confidence (i.e., the null hypothesis is rejected 99% of the time) it also means that only ~25% of the sea level variability is related to (not necessarily caused by) FC variability, since other forces like air pressure and wind (Piecuch and Ponte, 2015; Woodworth et al., 2016) have strong influence on sea level. A more detailed statistical analysis of the GS-WL correlations and the implications for predictability of coastal sea level are included in a recent study (Ezer and Atkinson, 2017). The daily change in transport is a good indicator for a sudden rise in WL (see the three peaks in WL between days 270–285 in Fig. 2c). Unfortunately, during Hurricane Hermine (which caused significant flooding in Norfolk) the FC cable did not record any data (days 243–252 in Fig. 2b). Analysis by Ezer et al. (2013) of a simple geostrophic balance of a barotropic current flowing along the coast show the two ways in which the GS can influence coastal sea level, explaining why both, the GS strength itself (Fig. 2b) through the change in the sea level slope across the current and changes in the GS flow (Fig. 2c) through on/offshore transport variations can be related to variations in coastal sea level.

During the period when Hurricane Matthew moved along the southeastern U.S. coast until it dissipated (October 7–12, 2016) coastal sea level rose from Florida to New Jersey, as shown by the tide gauge data and the model output (Fig. 3). The largest impact (and a more accurate model prediction) is seen in the SAB from Florida to North Carolina (hours 20–30), where direct storm surge was observed and predicted. An increased water levels in the MAB, as far north as Atlantic City can also be seen about 2 days later (hours 60–80), but the model did not accurately predict the timing and amplitude of the WL rise farther north. Model-data comparison of the maximum coastal sea level rise during those 5 days (Fig. 4) indicates that while the model may have captured the general pattern of sea level rise along the coast, the forecast underestimated the water level rise in most stations. This discrepancy is expected because of the idealized initialization and the fact that the ocean model component of the HWRF-POM system does not have high enough resolution and detailed coastal topography (compared with latest storm surge models).

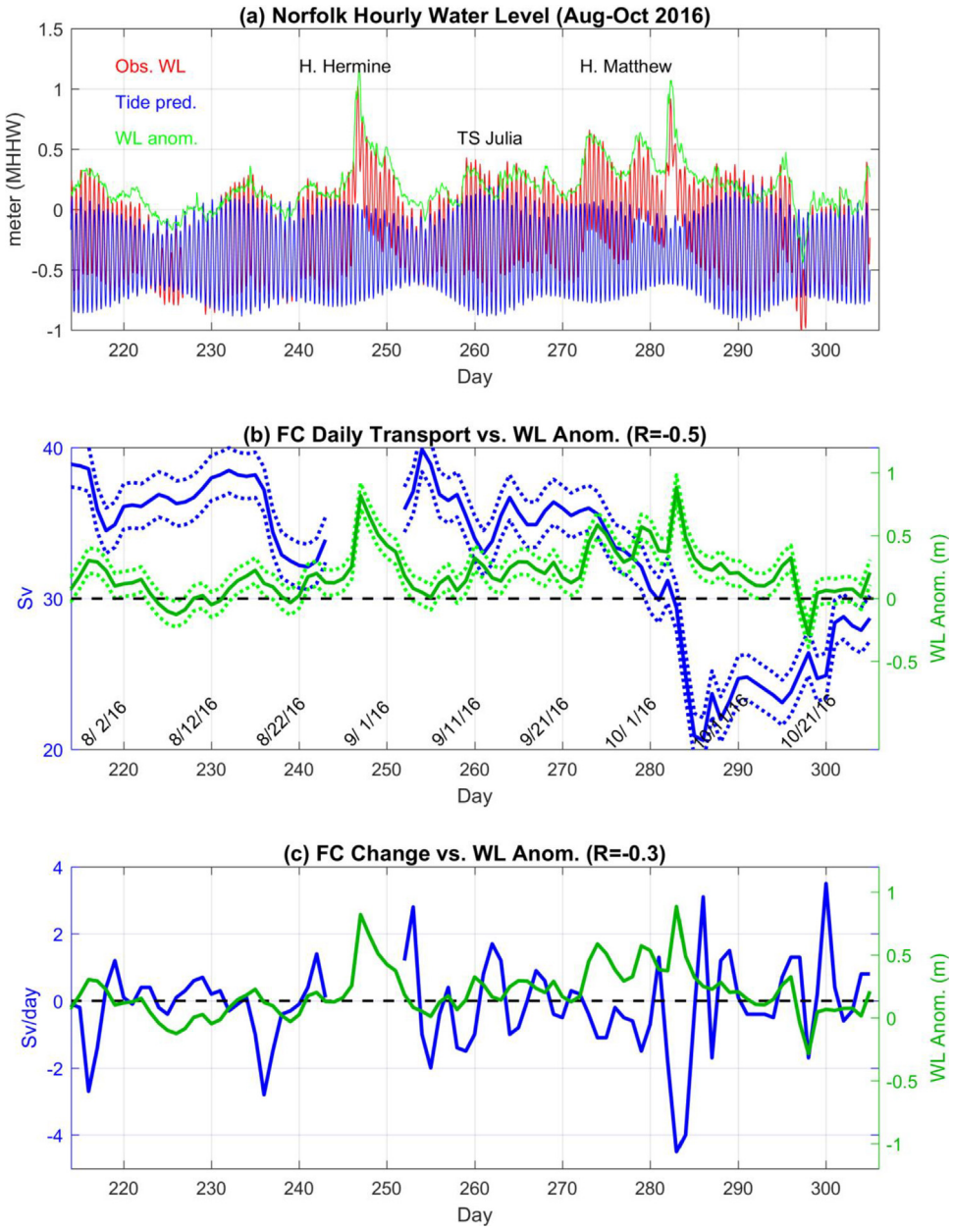

Fig. 2. (a) Hourly water level (WL) data (relative to Mean Higher High Water, MHHW) from the tide gauge at Sewells Point (Norfolk, VA; for location, see Fig. 1); red, blue and green lines represent the observations, the tidal prediction and the anomaly (observed-predicted), respectively. Also indicated are the periods when two hurricanes and a tropical storm were located offshore in the Atlantic (none of these storms came close to Norfolk). (b) Daily Florida Current (FC) transport from the cable across the Florida Strait (blue line, in Sv; dash lines are estimated errors) and the daily averaged WL in Norfolk (green line, in m; dash lines are estimated errors). (c) Same as (b), but for the FC transport change (in Sv per day). The correlation between WL and FC are indicated. Note that during Hurricane Hermine the FC cable stopped working (gap in days 243–252). (For interpretation of the references to colour in this figure legend, the reader is referred to the web version of this article.)

3.2. Impact of Hurricane Matthew on the Gulf Stream

Since there are no observations of the thermal and velocity fields throughout the water column during the passage of the hurricane, the model simulations are used to better understand the impact on the GS. Even if the operational model has some discrepancies with the real ocean, especially due to the initialization of subsurface fields, it can still provide a tool to better understand the mechanism involved. Fig. 5 demonstrates how the hurricane disrupts the GS flow structure in the Mid-Atlantic Bight (MAB; Fig. 5a and b) and in the South Atlantic Bight (SAB; Fig. 5c and d), and how temperatures change in the SAB during this period (Fig. 5e and f). It also shows the decrease of sea surface elevation gradient across the GS, while sea

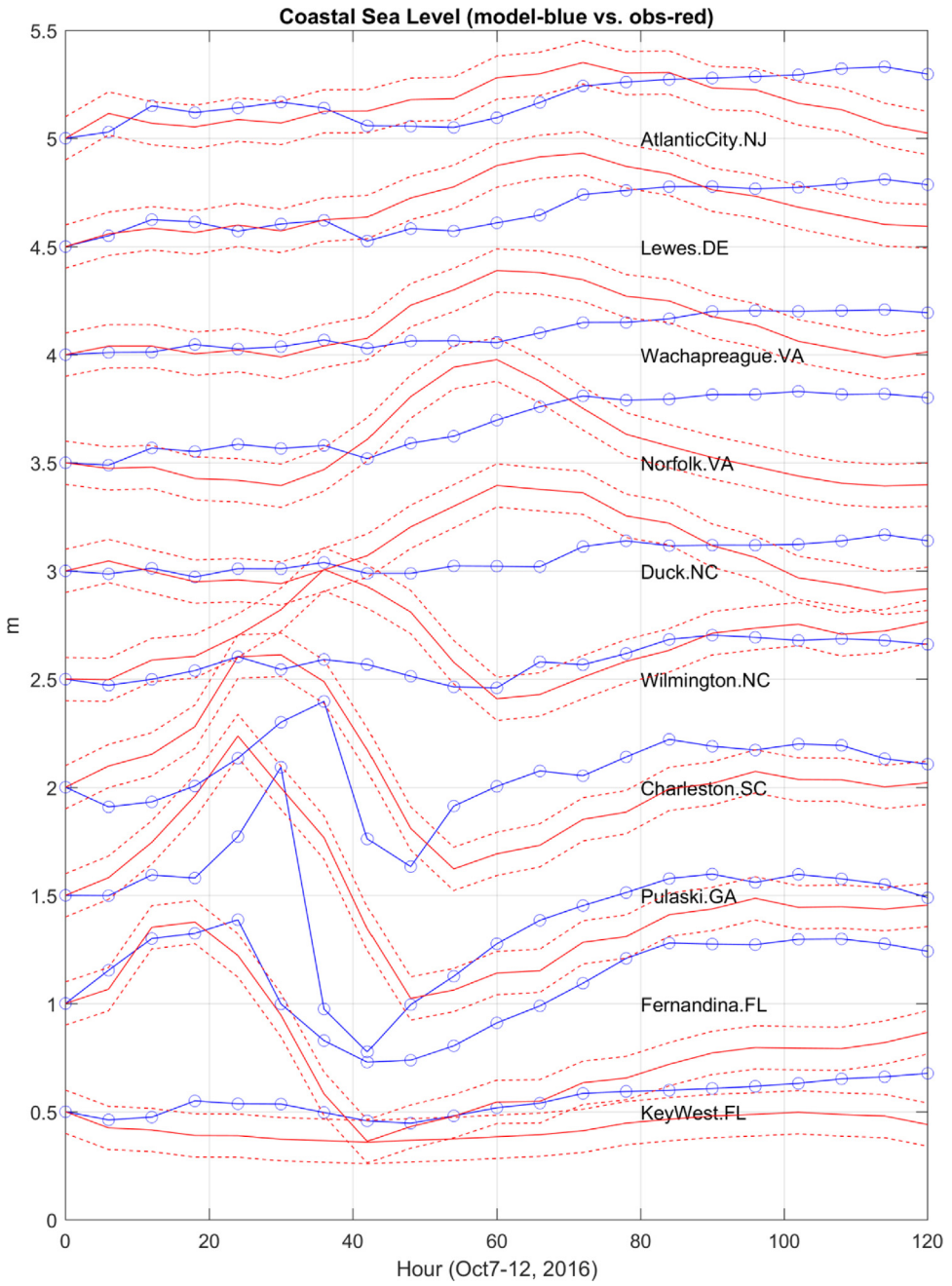

Fig. 3. Coastal sea level along the coast between October 7 and October 12, 2016 (6-hourly). Solid and dash red lines are the tide gauge data and the estimated errors, respectively (the tides were removed with a 24-h running filter). Blue lines and circles are from the model (at the model grid points closest to the tide gauges). Lines are vertically shifted for clarity with the locations arranged from north (top) to south (bottom); the stations are located at the following latitudes: 39.36°N, 38.78°N, 37.61°N, 36.95°N, 36.18°N, 34.23°N, 32.78°N, 32.03°N, 30.67°N and 24.56°N. (For interpretation of the references to colour in this figure legend, the reader is referred to the web version of this article.)

level was raised near the coast (gray area in all panels of Fig. 5). In the SAB (29°N; Fig. 5c and d) the impact of the hurricane is the most dramatic. At the beginning of the period when surface wind-driven currents are in the direction of the FC (Fig. 1b) a strong northward shallow flow is seen at the top ~70 m (Fig. 5c) which coincides with the depth of the thermocline (Fig. 5e). However, by October 12, after the hurricane already passed this area, the GS was weaker and deeper (to depth of ~500 m), and strong southward flow along the coast (blue in Fig. 5d) was accompanied by increased sea level toward the coast and upwelling of cold water is seen along the slope (Fig. 5f). A recent study of the impact of hurricanes on the GS extension north of Cape Hatteras shows a deepening of the mixed layer depth from 10 to 30 m (Kourafalou et al., 2016), but in comparison, the near coast impact seen here may be more complex as it involves additional coastal processes such as upwelling and

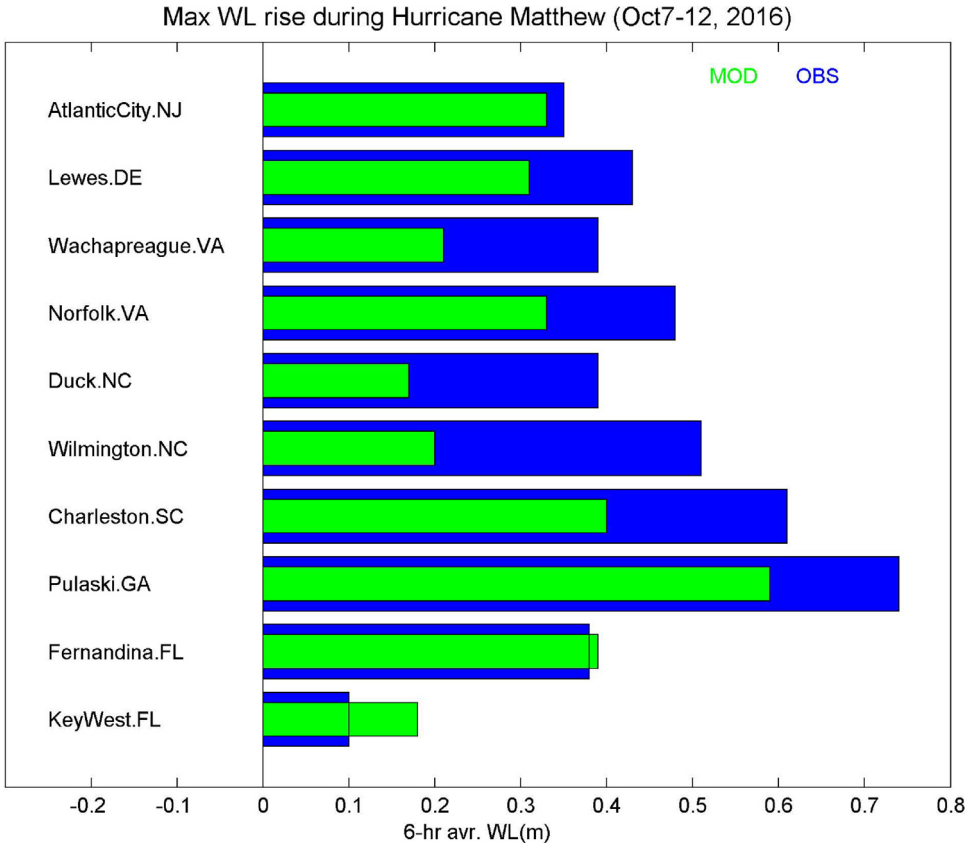

Fig. 4. Maximum water level rise (6-h averages) relative to October 7, 2016, for the locations in Fig. 3. Blue and green bars represent the observed and the model data, respectively. (For interpretation of the references to colour in this figure legend, the reader is referred to the web version of this article.)

coastal waves. It should also be noted that local ocean conditions such as stratification strength, currents direction and wind prior to the path of the storm could largely influence the amount of deepening of the mixed layer during the storm.

There are several potential ways in which the hurricane can influence ocean currents. First, direct wind-driven currents are generated near the surface due to the strong winds, this can be seen in Fig. 1b–d; this contribution will be marked as V_w ("w" for wind-driven). Second, the mixing induced by the wind and waves can disrupt the density field (i.e., Fig. 5) eroding the GS front and affecting the geostrophic component of the flow; this contribution will be marked as V_g ("g" for geostrophic). The geostrophic contribution to the surface flow can be estimated from the sea level slope, $(\Delta h/\Delta x)$ across the GS, $V_g = (g/f)(\Delta\eta/\Delta x)$, where g is gravity and f is the Coriolis parameter for that latitude (assuming the GS flows northward and is at first order in a geostrophic balance). The center of the GS can be defined as the location with the maximum surface slope. There are also other secondary impacts such as wind-driven Ekman transport to the right of the wind direction, potential upwelling/downwelling flows, internal and inertial waves and possibly GS meandering and eddies. However, for simplicity we assume that the surface flow in the model includes only two contributions, geostrophic and non-geostrophic flows, $V_s = V_g + V_w$. It is assumed here that the wind-driven component dominates the non-geostrophic flow. Fig. 6 shows how the three terms of the surface flow change over time for the center of the GS across three sections: the lower MAB (Fig. 6a), the central SAB (Fig. 6b) and in the Florida Strait (FS; Fig. 6c). The wind-driven portion is responsible for variations of $\sim$0.5 m s^{-1} in the FS (Fig. 6c), $\sim$1 m s^{-1} in the MAB (Fig. 6a), and as much as $\sim$2.5 m s^{-1} in the central SAB (Fig. 6b); the strongest response is in the first couple of days when the hurricane was located offshore the SAB. Note that in the first few days the wind blew mostly against the direction of the FC flow (the hurricane's eye was located east of the Florida Strait, so the anti-clockwise wind pattern implies a southwestward flow)- this contributed to weakening of the FC from hours 35–115, when the geostrophic portion of the flow (red line) shows a drop from $\sim$1.8 m s^{-1} to $\sim$0.9 m s^{-1} (Fig. 6c). This drop is consistent with the assumption that the mixing is eroding the density gradients under the GS. Another interesting result is the large oscillations in V_w that are seen first in the SAB (hours 10–50; Fig. 6b) and later in the MAB (hours 60–120; Fig. 6a). The amplitudes of those oscillations are comparable to the GS flow itself, and their period of $\sim$27, 25 and 20 h, for latitudes 27°N, 29°N and 36°N, respectively, match nicely the expected periods of inertial oscillations, $T = 2\pi/f$. The surface velocity is dominated by these wind-driven inertial oscillations during a period of $\sim$2–4 days. The trends in the geostrophic velocity in the SAB and MAB are quite different- an increase in V_g in the SAB as the GS structure recovers from the storm and the flow is

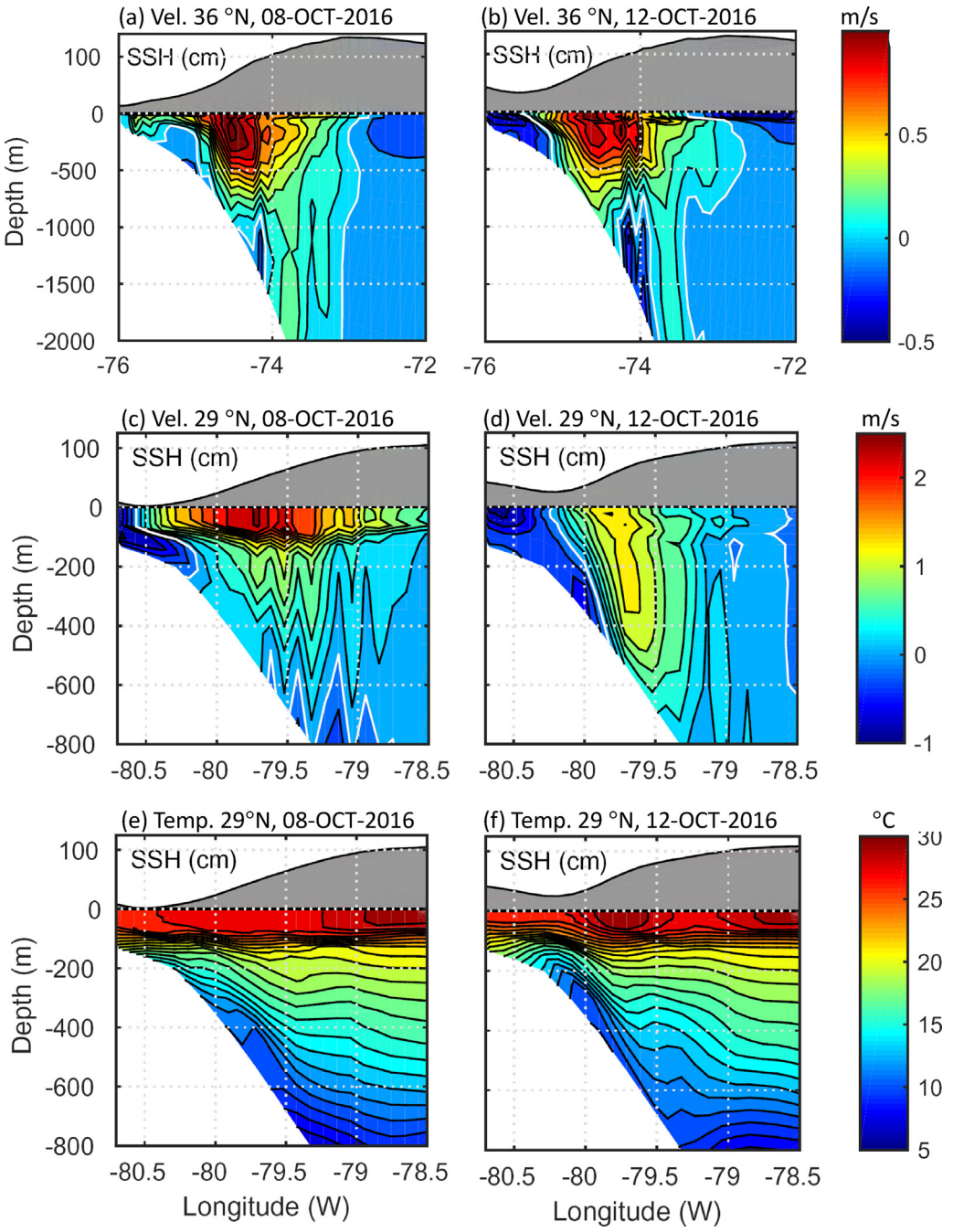

Fig. 5. East-west model cross-sections across the Gulf Stream for October 8 (left panels) and October 12 (right panels). From top to bottom are the northward velocity at 36°N (a and b) and at 29°N (c and d), and temperature at 29°N (e and f); white contour in the velocity plots indicate zero. Sea surface height (SSH in cm) is shown by the gray area.

adjusted to the change in the density field, while V_g is decreasing in the MAB when the impact of the storm reached farther north a few days later.

The GS transport is only directly measured at the Florida Straits (~27°N), but the model indicates that the impact of the hurricane extends farther downstream (~65°W, 38°N), with a decrease of ~20 Sv in the GS transport between October 8th and 12th as seen in the model stream function (Fig. 7). This model result is consistent with the ~20 Sv observed reduction of transport of the FC (Fig. 2b). Coherent large-scale variations in the GS transport along its path have been also indicated in other recent studies (Zhao and Johns, 2014; Domingues et al., 2016; Ezer, 2016), pointing to a mechanism involved fast moving barotropic waves adjustment that immediately spread a signal throughout the length of the GS. An additional

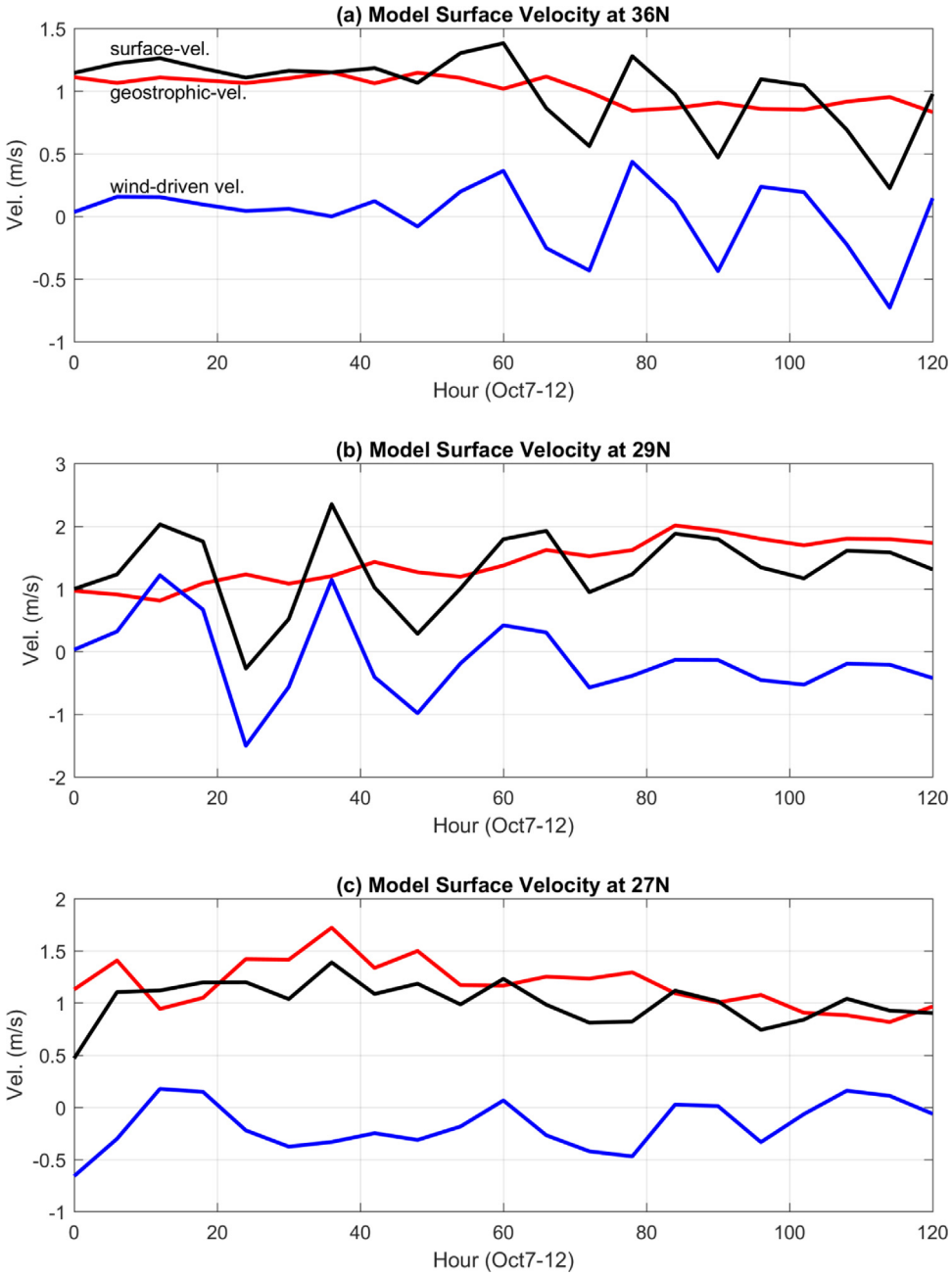

Fig. 6. Variations in model surface velocity across the Gulf Stream during October 7–12, 2016, at different latitudes: (a) 36°N (Mid-Atlantic Bight, just north of Cape Hatteras), (b) 29°N (South Atlantic Bight, off the Florida coast) and (c) 27°N (in the Florida Strait, off south Florida). Surface velocity V_s is in black, geostrophic velocity V_g (from the surface elevation slope) is in red and non-geostrophic velocity V_w (mostly "wind-driven") is in blue. The location of the Gulf Stream for each section is where surface elevation slope is maximum. (For interpretation of the references to colour in this figure legend, the reader is referred to the web version of this article.)

source of data that shows the impact of the storm is the sea surface height anomaly (SSHA) of satellite altimeter data (Fig. 8). When Matthew was just developing in the Caribbean Sea in late September, SSHA was mostly negative along the U.S. coast (including the Chesapeake Bay where Norfolk is located), but a few days after the storm moved away from the coast, the entire coast remains with anomalously high water and a continuous line of high SSHA is seen along the edge of the GS from Florida to the GS extension. Other satellite data can also be used to evaluate the coastal response and to look at the impact of the hurricane on changes in oceanic heat content (Oey et al., 2006, 2007), but here the altimeter data is only used qualitatively to demonstrate the spatial extent of the hurricane.

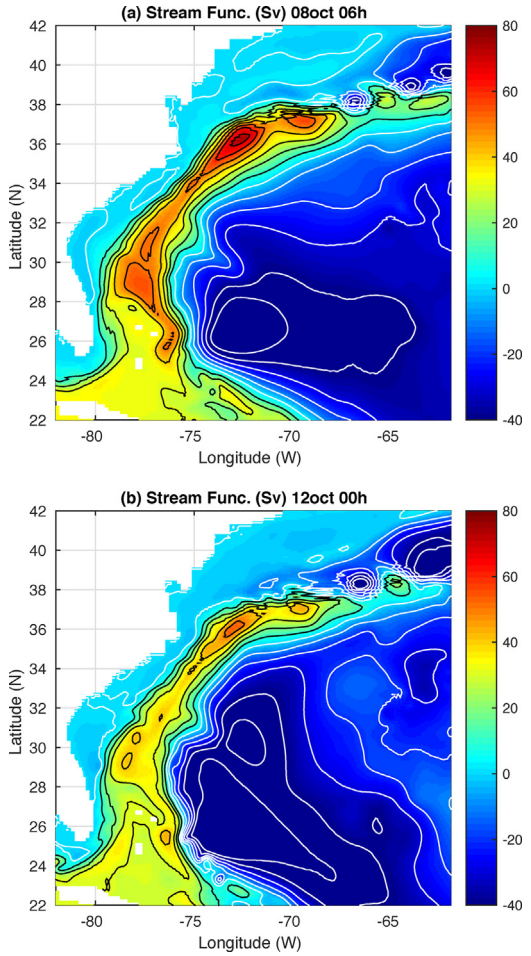

Fig. 7. Stream function calculated from the vertically averaged model velocity for (a) October 8 and (b) October 12. Contour interval is 10 Sv and black/white contours indicate positive/negative values.

Additional observations of surface currents are also available from several land-based HF coastal radars (Kohut et al., 2012). While these measurements aim to study and monitor surface currents on the shelf and in estuaries (Paduan et al., 2004), near Cape Hatteras, NC, the GS is close enough to the coast that the radar can capture part of the GS (Fig. 9a and b). After the hurricane passed the region, the surface currents across the GS are less organized and generally weaker. The maximum current speed across the GS declined from ~1.75 m s^{-1} in 6-October to ~1.5 m s^{-1} in 9-October and to as low as ~0.65 m s^{-1} in 11-October (Fig. 9c); the lowest velocities are about 50% of the typical surface velocity of the GS, and this decline is in line with the other observations shown before.

3.3. *Florida current variability and storms*

The various data sources describe here show a significant short-term impact on the GS from one storm (Hurricane Matthew, 2016). Anecdotal evidence from other storms such as Hurricane Sandy (2012) and Hurricane Joaquin (2015), show similar patterns of weakening GS and rising sea levels in wide coastal regions far away from the direct impact of the storm. Examples of GS-sea level correlation patterns similar to Fig. 2 (but for other years) can be found for example in Ezer and Atkinson (2014, 2015, 2017). Some questions that this study poses include: 1. How often do events of such a large temporary decline in the GS occur, and 2. Can these events influence the general variability of the GS and the seasonal pattern. Therefore, the daily FC transport record for 1982–2016 was analyzed (note a 1.5-year gap in the data during 1998–2000). Fig. 10a and b shows the histograms of the daily transport and the daily change in transport of the FC, respectively. Note the logarithmic scale to emphasize the extreme cases. It is clear that both histograms are not symmetric relative to the mean, with more cases of extremely weak or extreme weakening FC than cases with extremely strong FC. The FC weakening during Hurricane Matthew is very rare, outside 3 standard deviations; during ~35 years of data there were only ~20 days with similar or weaker FC. These rare events of very weak FC have a clear seasonal pattern (Fig. 10c and d), they occur mostly during the fall when hurricanes and tropical storms develop (October–November), sometimes during early spring (March–April) and

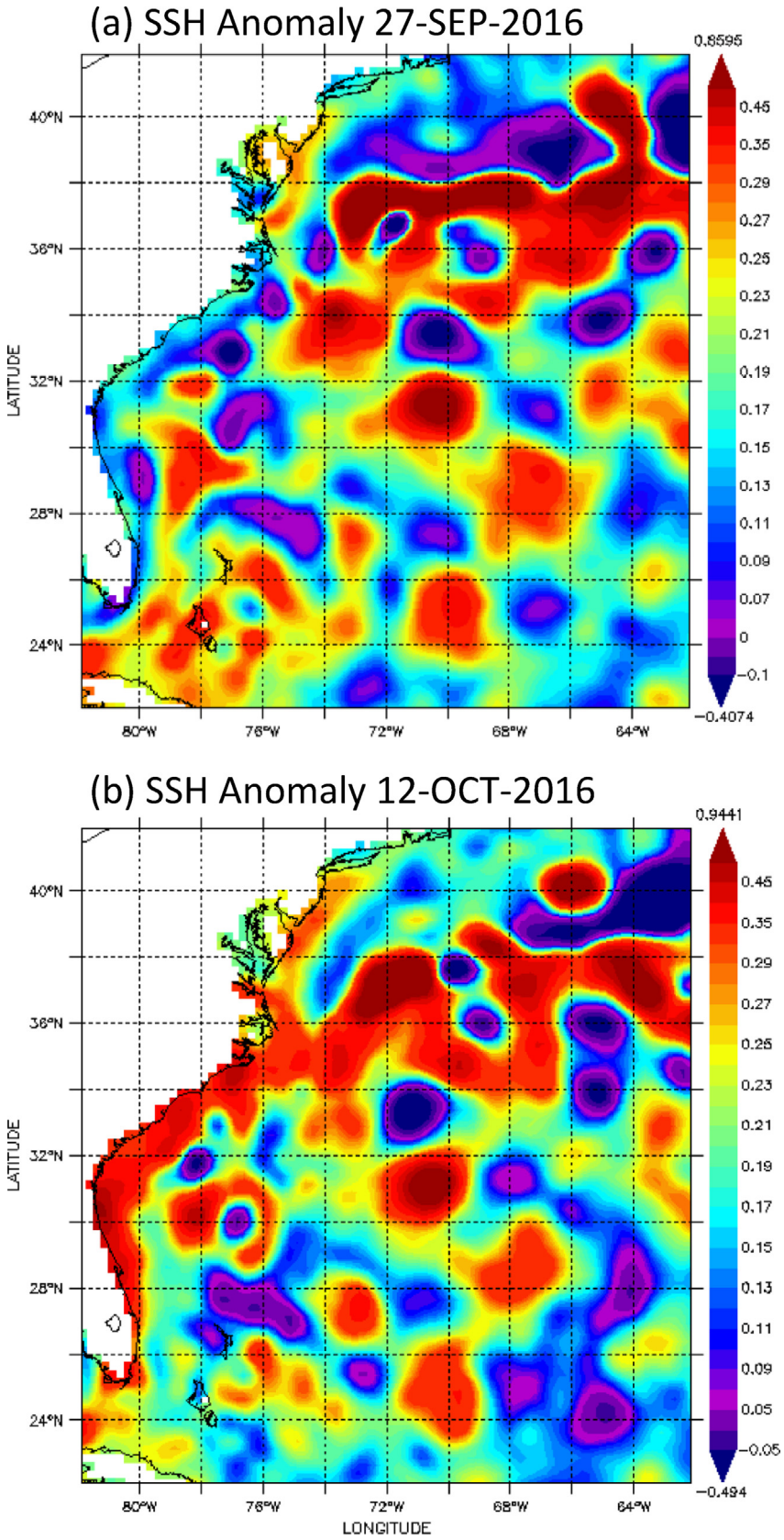

Fig. 8. Sea surface height anomaly (in m relative to the long-term mean SSH) from satellite altimetry data for (a) September 27, 2016 (before the storm reached the region) and (b) October 12, 2016 (after the storm dissipated and moved offshore).

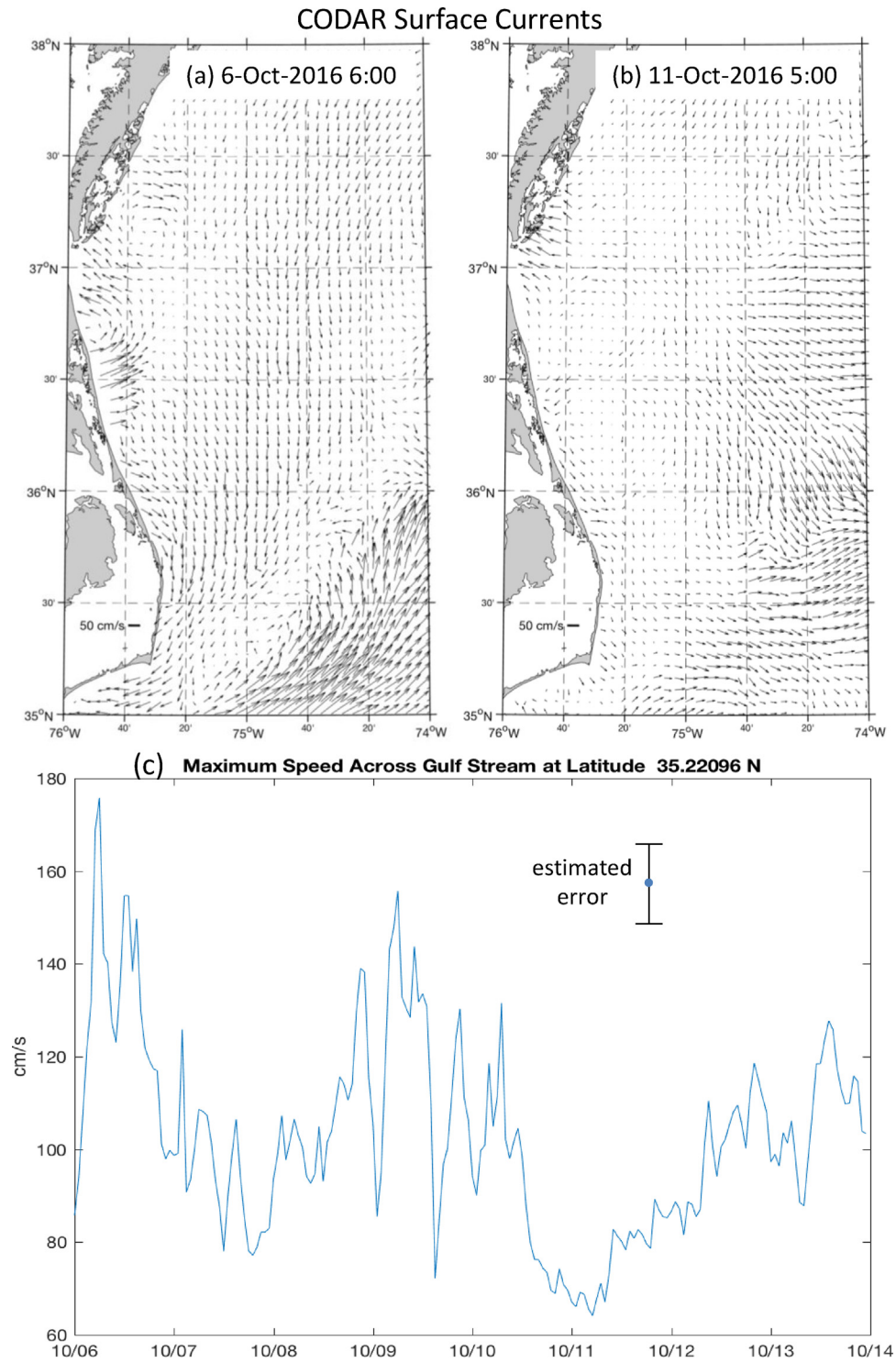

Fig. 9. Surface currents from CODAR for (a) October 6, 2016 at 06:00 and (b) October 11, 2016 at 05:00. (c) Time series of the maximum velocity speed across the Gulf Stream at 35.22°N. The vectors in (a) and (b) represent the time of maximum and minimum speed in (c).

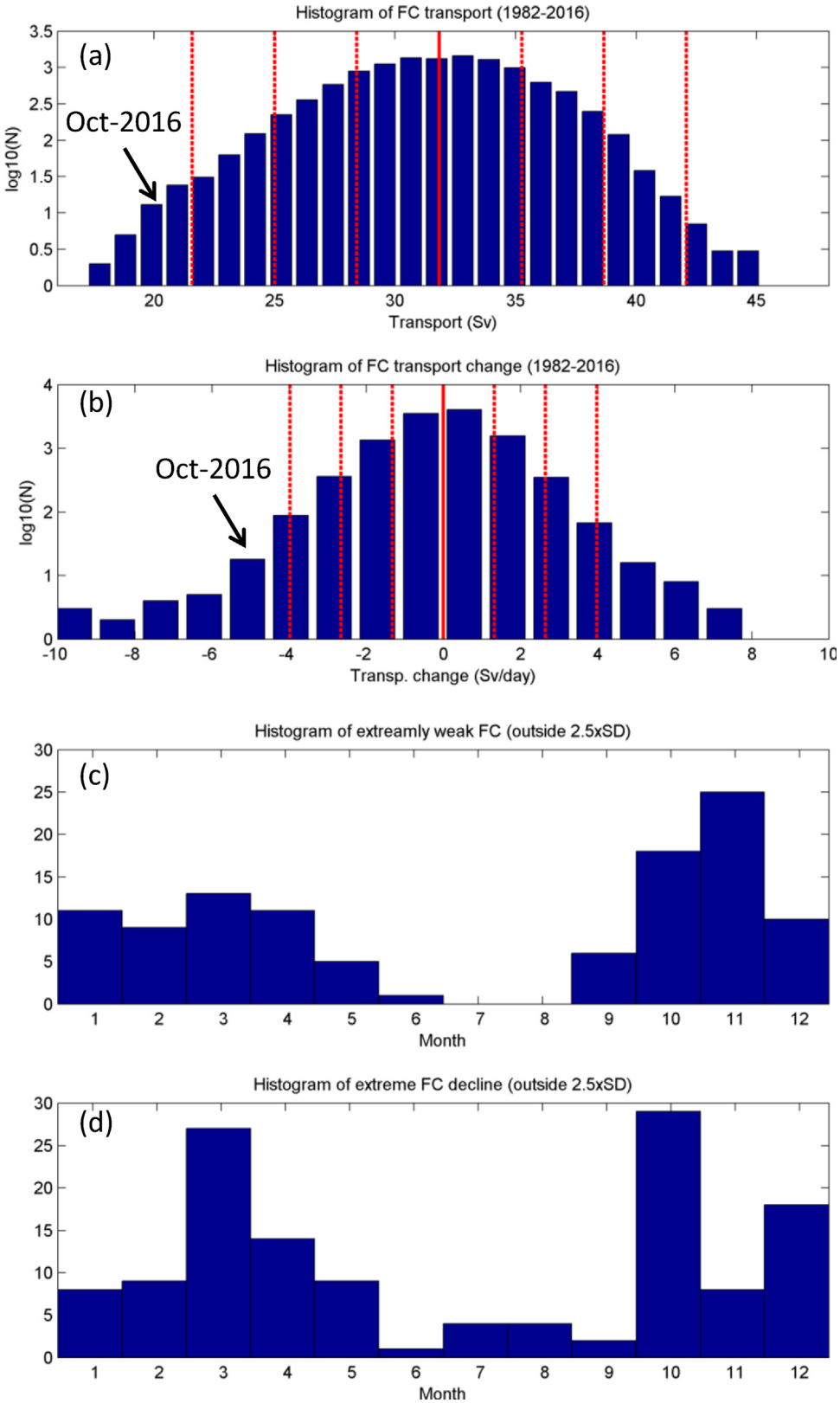

Fig. 10. Histograms of Florida Current observations for 1982–2016: (a) daily transports and (b) daily change in transport. Vertical dash lines represent 1, 2 and 3 standard deviation (SD) from the mean (solid red line); the vertical axis is logarithmic and the values during hurricane Matthew are indicated. Histograms of the monthly distribution of extremely weak FC (c) or extreme weakening in FC (d), when the values are smaller than mean-2.5SD. (For interpretation of the references to colour in this figure legend, the reader is referred to the web version of this article.)

almost never in the summer (June-August). More research is needed to statistically correlate this seasonal pattern in extreme FC events with the number of storms, their location relative to the GS and the duration they spent over the region. However, several individual cases of extremely weak FC coincide with the existence of nearby tropical storm or hurricane. Since storms do have a seasonal pattern, it is quite possible that they have some effect on the seasonal pattern of the FC, but this is a topic for further studies.

4. Summary and conclusions

Hurricane Matthew, which caused significant damage in the southeastern U.S. in October 2016, had quite an unusual path, hugging the coasts of Florida, Georgia, South Carolina and North Carolina without making a significant landfall and then looping eastward and away from the coast. Therefore, the hurricane stayed off the SAB coast for an unusually long period, having sufficient time to influence ocean currents and large stretches of coasts. In addition, flood damage farther north and well away from the direct influence of the storm happened when heavy rain was combined with high water levels that prevented draining of flooded streets. Based on past experience (Ezer and Atkinson, 2014, 2015, 2017; Ezer, 2016) it has been suggested that a weakening Gulf Stream following the storm may have contributed to high water levels in the MAB.

To evaluate the impact of the hurricane on the ocean, four different sources of data were analyzed: cable measurements across the Florida Straits that measured the FC transport, satellite altimeter data that measured SSHA, coastal HF radar that measured surface currents and output from the operational HWRF coupled hurricane-ocean model. All those data, including the model results, indicate that the hurricane caused a dramatic decline in the GS flow, it disrupted the thermal structure of the GS and increased coastal sea level along the path of the GS, even for locations out of the reach of the hurricane itself. The transport in the Florida Straits, the subsurface GS in the SAB and the MAB, as well as the surface GS currents off Cape Hatteras all declined by about 50% during a period of a few weeks, with a more dramatic decline within days during the period of the hurricane itself. The sea level rise along the coast from Florida to New Jersey combine both storm surge in the vicinity of the storm in the SAB, as well as indirect contribution from the weakening of the GS and the reduction of sea level gradients across the stream. The impact of the storm lasted for several days after the storm passed, as the baroclinic structure of the GS recovered from the disruption. Analysis of the model simulations helped to separate between changes in the geostrophic velocity and non-geostrophic (mostly wind-driven) velocity. The wind-driven component includes the generation of inertial oscillations with velocities comparable to the GS itself ($\sim$1 m s^{-1}).

In view of the variability of the observed daily FC since 1982, extreme events (when the FC transport is below 20 Sv or the daily decline is 4 Sv or more) occur quite rarely, outside 3 standard deviations from the mean. These events have clear seasonal pattern (more extreme weak FC events in October-November) that suggests a possible contribution to the seasonal variability of the FC transport with lower transport during the hurricane season. Monthly mean FC transport since 1982 (not shown) indicates a difference between the maximum mean transport (in July) and the minimum transport (in November) of $\sim$3 Sv (this is slightly different than the seasonal cycle of the first 16 years with a minimum in January, as reported by Baringer and Larsen, 2001). However, if variations outside 1 standard deviation are excluded, the amplitude of the seasonal FC transports is only $\sim$1 Sv. This difference is not statistically significant, but points to the possibility that extreme events may contribute to the seasonal cycle. Moreover, interannual variations in the number, intensity and path of tropical storms can add to other interannual influences on the FC, such as the impact of the North Atlantic Oscillations and remote forcing (Domingues et al., 2016). In addition to the ocean dynamic influence, the low atmospheric pressure near storms can also impact variations in sea level (short-term and long-term) through the inverted barometer effect (Piecuch and Ponte, 2015). This study adds to the growing evidence that remote influence on coastal sea level from variations in ocean circulation is an important factor that should be considered in prediction models.

Acknowledgements

Old Dominion University's Climate Change and Sea Level Rise Initiative (CCSLRI) provided partial support for this study and the Center for Coastal Physical Oceanography (CCPO) provided computational support. The hourly tide gauges sea level data are available from: (http://opendap.co-ops.nos.noaa.gov/dods/). The Florida Current transport record is obtained from: http://www.aoml.noaa.gov/phod/floridacurrent/. The altimeter data are obtained from AVISO (http://las.aviso.oceanobs.com/las/). The HWRF model results are available from NOAA/NCEP (http://www.emc.ncep.noaa.gov/gc_wmb/vxt/HWRF/), and we thank the URI's hurricane group for providing us with output from the POM component of HWRF model. The CODAR data are available from http://tds.marine.rutgers.edu/thredds/cool/codar/, and we thank Teresa Updyke for providing us with the data and making the plots.

References

AVISO, 2009. SSALTO/DUACS User Handbook: (M)SLA and (M)ADT Near-real Time and Delayed Time Products. Rep. CLS-DOS-NT, vol. 6., pp. 51.

Baringer, M.O., Larsen, J.C., 2001. Sixteen years of florida current transport at 27°N. Geophys. Res. Lett. 28 (16), 3179–3182, http://dx.doi.org/10.1029/2001GL013246.

Bender, M.A., Ginis, I., 2000. Real-case simulations of hurricane–ocean interaction using a high-resolution coupled model: effects on hurricane intensity. Mon. Wea. Rev. 128, 917–946, http://dx.doi.org/10.1175/1520-0493(2000)128<0917:RCSOHO>2.0.CO;2.

Blaha, J.P., 1984. Fluctuations of monthly sea level as related to the intensity of the Gulf Stream from Key West to Norfolk. J. Geophys. Res. Oceans 89 (C5), 8033–8042.
Boon, J.D., 2012. Evidence of sea level acceleration at U.S. and Canadian tide stations, Atlantic coast, North America. J. Coast. Res. 28 (6), 1437–1445, http://dx.doi.org/10.2112/JCOASTRES-D-12-00102.1.
Domingues, R., Baringer, M., Goni, G., 2016. Remote sources for year-to-year changes in the seasonality of the Florida Current transport. J. Geophys. Res. 121 (10), 7547–7559, http://dx.doi.org/10.1002/2016JC012070.
Ezer, T., Atkinson, L.P., 2014. Accelerated flooding along the U.S. East Coast: on the impact of sea-level rise, tides, storms, the Gulf Stream, and the North Atlantic Oscillations. Earth's Future 2 (8), 362–382, http://dx.doi.org/10.1002/2014EF000252.
Ezer, T., Atkinson, L.P., 2015. Sea level rise in Virginia–causes, effects and response. Virginia J. Sci. 66 (3), 355–359, Publication of the Virginia Academy of Science.
Ezer, T., Atkinson, L.P., 2017. On the predictability of high water level along the U.S. East Coast: can the Florida Current measurement be an indicator for flooding caused by remote forcing? Ocean Dyn. 67 (6), 751–766, http://dx.doi.org/10.1007/s10236-017-1057-0.
Ezer, T., Corlett, W.B., 2012. Is sea level rise accelerating in the Chesapeake Bay? A demonstration of a novel new approach for analyzing sea level data. Geophys. Res. Lett. 39, L19605, http://dx.doi.org/10.1029/2012GL053435.
Ezer, T., Atkinson, L.P., Corlett, W.B., Blanco, J.L., 2013. Gulf Stream's induced sea level rise and variability along the U.S. mid-Atlantic coast. J. Geophys. Res. 118, 685–697, http://dx.doi.org/10.1002/jgrc.20091.
Ezer, T., 2001. Can long-term variability in the Gulf Stream transport be inferred from sea level? Geophys. Res. Lett. 28 (6), 1031–1034, http://dx.doi.org/10.1029/2000GL011640.
Ezer, T., 2013. Sea level rise, spatially uneven and temporally unsteady: why the U.S. East Coast, the global tide gauge record, and the global altimeter data show different trends. Geophys. Res. Lett. 40, 5439–5444, http://dx.doi.org/10.1002/2013GL057952.
Ezer, T., 2015. Detecting changes in the transport of the Gulf Stream and the Atlantic overturning circulation from coastal sea level data: the extreme decline in 2009–2010 and estimated variations for 1935–2012. Glob. Planet. Change 129, 23–36, http://dx.doi.org/10.1016/j.gloplacha.2015.03.002.
Ezer, T., 2016. Can the Gulf Stream induce coherent short-term fluctuations in sea level along the U.S. East Coast? A modeling study. Ocean Dyn. 66 (2), 207–220, http://dx.doi.org/10.1007/s10236-016-0928-0.
Goddard, P.B., Yin, J., Griffies, S.M., Zhang, S., 2015. An extreme event of sea-level rise along the Northeast coast of North America in 2009–2010. Nat. Commun. 6 (6345), http://dx.doi.org/10.1038/ncomms7346.
Kohut, J., Roarty, H., Randall-Goodwin, E., Glenn, S., Lichtenwalner, C.S., 2012. Evaluation of two algorithms for a network of coastal HF radars in the Mid-Atlantic Bight. Ocean Dyn. 62 (6), 953–968, http://dx.doi.org/10.1007/s10236-012-0533-9.
Kourafalou, V.H., Androulidakis, Y.S., Halliwell, G.R., Kang, H.S., Mehari, M.M., Le Hénaff, M., Atlas, R., Lumpkin, R., 2016. North Atlantic Ocean OSSE system development: nature Run evaluation and application to hurricane interaction with the Gulf Stream. Prog. Oceanogr. 148, 1–25, http://dx.doi.org/10.1016/j.pocean.2016.09.001.
Li, Y., Xue, H., Bane, J.M., 2002. Air-sea interactions during the passage of a winter storm over the Gulf Stream: a three-dimensional coupled atmosphere-ocean model study. J. Geophys. Res. 107, C11, http://dx.doi.org/10.1029/2001JC001161.
Liu, X., Wei, J., 2015. Understanding surface and subsurface temperature changes induced by tropical cyclones in the Kuroshio. Ocean Dyn. 65, 1017, http://dx.doi.org/10.1007/s10236-015-0851-9.
McCarthy, G., Frejka-Williams, E., Johns, W.E., Baringer, M.O., Meinen, C.S., Bryden, H.L., Rayner, D., Duchez, A., Roberts, C., Cunningham, S.A., 2012. Observed interannual variability of the Atlantic meridional overturning circulation at 26.5°N. Geophys. Res. Lett. 39 (19), s1, http://dx.doi.org/10.1029/2012GL052933.
Meinen, C.S., Baringer, M.O., Garcia, R.F., 2010. Florida Current transport variability: an analysis of annual and longer-period signals. Deep Sea Res. 57 (7), 835–846, http://dx.doi.org/10.1016/j.dsr.2010.04.001.
Oey, L.-Y., Ezer, T., Wang, D.P., Fan, S.J., Yin, X.Q., 2006. Loop current warming by hurricane wilma. Geophys. Res. Lett. 33, L08613, http://dx.doi.org/10.1029/2006GL025873.
Oey, L.-Y., Ezer, T., Wang, D.-P., Yin, X.Q., Fan, S.-J., 2007. Hurricane-induced motions and interaction with ocean currents. Cont. Shelf Res. 27, 1249–1263, http://dx.doi.org/10.1016/j.csr.2007.01.008.
Paduan, J.D., Kosro, P.M., Glenn, S.M., 2004. A national coastal ocean surface current mapping system for the United States. Mar. Technol. Soc. J. 38 (2), 102–108, http://dx.doi.org/10.4031/002533204787522839.
Park, J., Sweet, W., 2015. Accelerated sea level rise and Florida current transport. Ocean Sci. 11, 607–615, http://dx.doi.org/10.5194/os-11-607-2015.
Piecuch, C.G., Ponte, R.M., 2015. Inverted barometer contributions to recent sea level changes along the northeast coast of North America. Geophys. Res. Lett. 42, 5918–5925, http://dx.doi.org/10.1002/2015GL064580.
Piecuch, C.G., Dangendorf, S., Ponte, R., Marcos, M., 2016. Annual sea level changes on the North American Northeast Coast: influence of local winds and barotropic motions. J. Clim. 29, 4801–4816, http://dx.doi.org/10.1175/JCLI-D-16-0048.1.
Sallenger, A.H., Doran, K.S., Howd, P., 2012. Hotspot of accelerated sea-level rise on the Atlantic coast of North America. Nat. Clim. Change 2, 884–888, http://dx.doi.org/10.1038/NCILMATE1597.
Shay, L.K., Goni, G.J., Black, P.G., 2000. Effects of a warm oceanic feature on hurricane Opal. Mon. Weather Rev. 128, 1366–1383, http://dx.doi.org/10.1175/1520-0493(2000)128<1366:EOAWOF>2.0.CO;2.
Smeed, D.A., McCarthy, G., Cunningham, S.A., Frajka-Williams, E., Rayner, D., Johns, W.E., Meinen, C.S., Baringer, M.O., Moat, B.I., Duchez, A., Bryden, H.L., 2013. Observed decline of the Atlantic Meridional Overturning Circulation 2004–2012. Ocean Sci. Discus. 10, 1619–1645, http://dx.doi.org/10.5194/osd-10-1619-2013.
Tallapragada, V., Bernardet, L., Biswas, M.K., Gopalakrishnan, S., Kwon, Y., Liu, Q., Marchok, T., Sheinin, D., Tong, M., Trahan, S., Tuleya, R., Yablonsky, R., Zhang, X., 2014. Hurricane weather research and forecasting (HWRF) model: 2014 scientific documentation. In: Bernardet, L. (Ed.), NCAR Development Tested Bed Center Report. , 81 pp.
Wdowinski, S., Bray, R., Kirtman, B.P., Wu, Z., 2016. Increasing flooding hazard in coastal communities due to rising sea level: case study of Miami Beach, Florida. Ocean Coast. Manage. 126, 1–8, http://dx.doi.org/10.1016/j.ocecoaman.2016.03.002.
Woodworth, P.L., Maqueda, M.M., Gehrels, W.R., Roussenov, V.M., Williams, R.G., Hughes, C.W., 2016. Variations in the difference between mean sea level measured either side of Cape Hatteras and their relation to the North Atlantic Oscillation. Clim. Dyn., 1–19, http://dx.doi.org/10.1007/s00382-016-3464-1.
Wu, C.-R., Chang, Y.-L., Oey, L.-Y., Chang, C.W.J., Hsin, Y.C., 2008. Air-sea interaction between tropical cyclone Nari and Kuroshio. Geophys. Res. Lett. 31, L12605, http://dx.doi.org/10.1029/2008GL033942.
Yablonsky, R.M., Ginis, I., Thomas, B., Tallapragada, V., Sheinin, D., Bernardet, L., 2015. Description and analysis of the ocean component of NOAA's operational Hurricane Weather Research and Forecasting (HWRF) Model. J. Atmos. Oceanic Technol. 32, 144–163, http://dx.doi.org/10.1175/JTECH-D-14-00063.1.
Zhao, J., Johns, W.E., 2014. Wind-forced interannual variability of the atlantic meridional overturning circulation at 26.5°N. J. Geophys. Res. Oceans 119, 6253–6273, http://dx.doi.org/10.1002/2013JC009407.